Nat Hazards (2015) 78:1091–1110
DOI 10.1007/s11069-015-1758-y

ORIGINAL PAPER

Coda wave attenuation characteristics for the Bilaspur region of Himachal Lesser Himalaya

Vandana[1] · S. C. Gupta[1] · Ashwani Kumar[1]

Received: 6 November 2014 / Accepted: 11 April 2015 / Published online: 24 April 2015

Abstract Seismic wave attenuation is one of the most important parameters that reflect characteristics of the medium traversed by the seismic waves. This parameter is essential for many studies such as determining earthquake source parameters, predicting earthquake strong ground motion, monitoring nuclear explosions and estimating seismic hazard. Since 1995, several region-specific attenuation relations have been developed for the Indian regions, but no such relation is available for the Bilaspur region of the Himachal Lesser Himalaya for the want of data. A six-station local seismological network, deployed in the environs of Koldam site, provided digital recordings of 41 local events occurred in the region from May 2013 to March 2014. This data set has been used to develop the attenuation relations for the region. Majority of the events occurred in the Himachal Lesser Himalaya between the main boundary thrust and the main central thrust. All events have epicentral distances <100 km and magnitudes between 0.5 and 2.9. Adopting the single backscattering model of Aki and Chouet (J Geophys Res 80:3322–3342, 1975), coda-Q (Q_c) of the region has been estimated in lapse time windows of 20, 30 and 40 s, respectively. For 30-s lapse time window, the attenuation follows the relation $Q_c(f) = (70.3 \pm 20.27) f^{(1.23 \pm 0.05)}$ for the region. The observed Q_c relation is compared with similar relations for seismically active Indian regions and some of the globally available relations. It is found that the average variation of Q_c for the Bilaspur region is very close to Amazon Craton (Brazil) due to similar lithologic setup. The variation of 'Q_0' and 'n' values indicates that the region is highly heterogeneous and seismically active. The region is more heterogeneous near the surface as compared to depth. The estimated Q_c relations can be utilized for computing source parameters of the local earthquakes and for seismic hazard assessment for the Bilaspur region of Himachal Lesser Himalaya.

Keywords Coda wave · Lapse time · Attenuation · Scattering · Himachal Lesser Himalaya

✉ Vandana
vandana.ghangas@gmail.com

[1] Department of Earthquake Engineering, IIT Roorkee, Roorkee, India

1 Introduction

The observed earthquake ground motions, in terms of amplitudes and frequency content, at recording sites, are influenced by the source, path and site characteristics. The effects of travel path on earthquake ground motion depend on the attenuation characteristics of the medium through which the seismic waves propagate; attenuation is an important parameter that governs the amplitudes and frequency content observed on the seismograms. The knowledge of the attenuation of seismic waves is essential for determining earthquake source parameters, predicting the strong ground motions due to earthquakes and estimating the seismic hazard of a region. This attenuation can be quantitatively defined by the inverse of the dimensionless quantity known as quality factor Q, which is a ratio of stored energy to dissipated energy during one cycle of the wave (e.g., Johnston and Toksöz 1981). The seismic wave attenuation is attributed to three factors: (1) anelastic absorption that mainly depends on temperature, fluid content and chemical compositions; (2) scattering of seismic waves, which is ascribed to generated small-scale velocity fluctuations; and (3) focusing of seismic waves due to propagation in 3-D structures. Because of these factors, amplitudes of seismic waves decay faster than predicted by geometrical spreading of wave fronts (Pandit et al. 2011). Therefore, attenuation provides important information about the structure of the earth (Calvet et al. 2013). Mak et al. (2004) observed that for high Q values ($Q > 600$) the region is tectonically stable, while for low Q values ($Q < 200$) the region is seismically active, and for Q values between (200 and 600), the region possesses moderate tectonic activity.

Due to the presence of various scale inhomogeneities in the earth, the observed ground motions in the vicinity of earthquakes often decay slowly leaving a coda following the direct, body and surface waves. These coda waves of local earthquakes were interpreted as backscattering waves from numerous randomly distributed heterogeneities in the earth crust (e.g., Aki 1969; Aki and Chouet 1975; Rautian 1976). The models were developed to use coda waves for the estimation of attenuation relations. The single scattering model considered the scattering as a weak process without loss of seismic energy by scattering, whereas the multiple scattering model the seismic energy transfer considered as a diffused process. Using coda waves, numerous studies have been conducted to determine the attenuation relation for different regions of the world (Ambeh and Fairhead 1989; Catherine 1990; Atkinson and Meeru 1992; Mandal and Rastogi 1998; Gupta et al. 1998; Mandal et al. 2001; Gupta and Kumar 2002; Paul et al. 2003; Kumar et al. 2005, 2007; Sharma et al. 2008; Sahin 2008; Raghukanth and Semala 2009; Dobrynina 2011; Gupta et al. 2012 and Calvet et al. 2013). Mukhopadhyay et al. (2006) computed the intrinsic and scattering attenuation characteristics using the coda waves of local earthquakes for the northwest Himalayas. Sato and Fehler (1998) estimated that the heterogeneities in the lithosphere were observed from coda-Q from local earthquakes on the scale of 0.1–10 km.

Himalaya, the highest mountain chain on the earth, is characterized by the concentration of interplate seismicity and high rate of upliftment as well as convergence (Molnar and Chen 1983; Nakata 1989; Demets et al. 1990). Himachal Lesser Himalaya, forming part of the northwest Himalaya, is bound to the west by the Kashmir Himalaya and to the east by the Garhwal Himalaya. Because of non-availability of digital data set, limited work has been carried out to estimate attenuation properties of the medium. A six-station local network of sensitive digital seismographs has been deployed in the Bilaspur region. The digital recordings from this network have been used to estimate the quality factor of the lithosphere of the Bilaspur region.

1.1 Geology, tectonics and seismicity of the Himachal Lesser Himalaya

The formation of the Himalaya has been attributed to the continent–continent convergence of the India and Eurasia lithospheric plates (e.g., Le Fort 1975; Seeber et al. 1981). From geological considerations, the Himalaya has been segregated into six parts: (1) the first part comprises basement rocks, (2) the second part represents inner crystalline nappe, (3) the third part is composed of rock types belonging to Simlas and Jaunsars, (4) the rock formations primarily belonging to Blainis, infra-Krols, Krols, Shalis and Tals constitute fourth part, (5) the lower tertiary containing rock formations like Subathus, Dagshais and Kasaulis comprises fifth part and (6) the sixth part represents sedimentary formations belonging to Siwalik group (e.g., Saxena 1971). The Himalaya is divided into four tectonic domains viz., the Sub-Himalaya (Siwalik), the Lesser Himalaya, the Great Himalaya and the Tethys Himalaya or Tibet Himalaya. The Indus-Tsangpo suture zone (ITSZ) constitutes the northern boundary of the India plate. Trans-Himadri fault defines the boundary between the Tethys Himalaya and the Great Himalaya. This fault was earlier called the Malari Thrust (Valdiya 1979; Valdiya et al. 1984) and later on renamed as Trans-Himadri fault (Valdiya 1987, 1989). The main central thrust (MCT) defines the boundary of the Great Himalaya and the Lesser Himalaya. The main boundary thrust (MBT) constitutes the boundary between the Lesser Himalaya and the Sub-Himalaya. The Himalaya frontal thrust (HFT) is located to the south of the Sub-Himalaya and separates it from the Indo-Gangetic Plains. The region between the MBT and the HFT is traversed by several subsidiary thrusts such as the Jawalamukhi Thrust (JT) and the Drang Thrust (DT). Within the above tectonic background, the study area is located in the Himachal Lesser Himalaya that forms the northwestern part of the Himalaya. Figure 1b depicts the segments of the MCT and the MBT, along with several other local tectonic features mapped in the study area. The tectonic features located in the close proximity of the Koldam site include the DT and the MBT. Geological mapping has indicated that at several places the MBT and the JT exhibited neotectonic activity (e.g., Srikanita and Bhargava 1998).

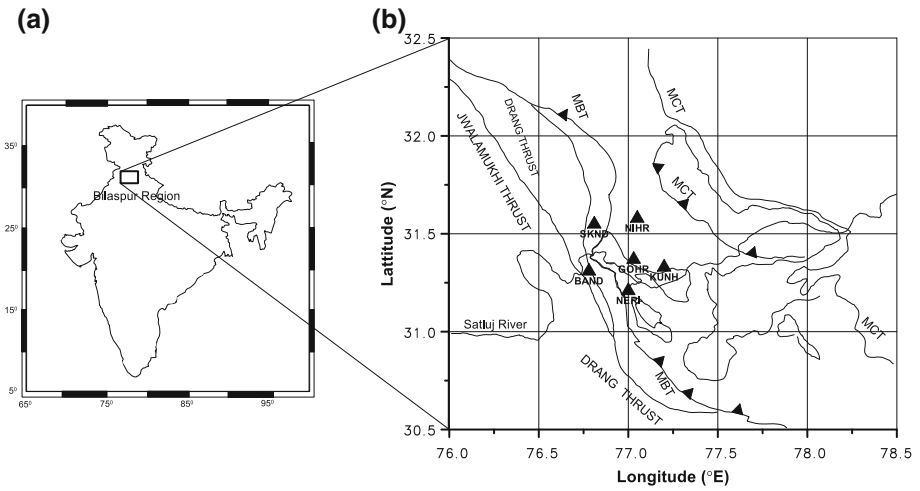

Fig. 1 **a** Map of India showing the study region (*rectangular box*). **b** Map showing tectonic features around Bilaspur region of the Himachal Lesser Himalaya (After GSI 2000). Tectonic features (*lines*) are shown and include: MBT; MCT; DT; JT. *Filled triangles* depict the network stations

The earthquake activity of the region is primarily ascribed to the convergence of the Indian and Eurasian tectonic plates. The study region falls in seismic zone V as per the seismic zoning map of India (IS: 1893-(Part l) 2002: General Provisions and Buildings). The region has witnessed many moderate- to large-sized earthquakes in the last more than 100 years. Prominent earthquakes that occurred in the Himachal Lesser Himalaya encompassing the Bilaspur region are listed in Table 1.

2 Methodology

This methodology adopted to estimate the quality factor (Q) of the Bilaspur region is based on well-known single backscattering model (Aki and Chouet 1975). This model is based on the premise that coda waves are backscattered body waves generated by randomly distributed heterogeneities in the earth's crust and upper mantle. The size of scatterers is considered greater than the wavelength, and no velocity change or multiple scattering is allowed in the medium. Kopnichev (1977) and Gao et al. (1983) demonstrated that the coda waves observed at short lapse times (<100 s) are because of the single scattering, whereas those at long lapse times (>100 s) are due to multiple scattering. Based on the

Table 1 Prominent earthquakes occurred in the Himachal Lesser Himalaya encompassing the Bilaspur region

Date	Place	Locations				References
		Latitude (°N)	Longitude (°E)	Intensity	Magnitude	
April 4, 1905	Kangra, Himachal Pradesh	32.3	76.2	10	$M_s = 7.8$	Ambraseys and Bilham (2000)
February 28, 1906	Kullu, Himachal Pradesh	32.0	77.0	na	$M_w = 6.4$	Thakur et al. (2014)
May 11, 1930	East of Sultanpur, Himachal Pradesh	31.7	77.0	na	$T_S = 6.0$	Thakur et al. (2014)
June 22, 1945	Chamba, Himachal Pradesh	32.6	75.9	9	$M_s = 7.5$	Srivastava et al. (1987)
September 12, 1951	Chamba–Udhampur Districts, Himachal Pradesh	33.3	76.5	na	$T_S = 6.0$	Thakur et al. (2014)
June 17, 1955	Lahaul–Spiti Districts, Himachal Pradesh	32.5	78.6	na	$T_S = 6.0$	Thakur et al. (2014)
January 19, 1975	Kinnaur, Himachal Pradesh	32.3	78.5	9	$M_s = 7.5$	Singh et al. (1976)
April 26, 1986	Dharmashala, Himachal Pradesh	32.1	76.4	6	$M_s = 5.0$	Kumar and Mahajan (1990)

single backscattering model, the coda wave amplitude $A(f, t)$ for a narrow bandwidth signal centered at frequency f and at lapse time t is given as (Aki and Chouet 1975):

$$A(f,t) = S(f)t^{-\alpha}\exp\left(\frac{-\pi f t}{Q_c}\right) \quad (1)$$

where $S(f)$ represents the source function at frequency f, α is the geometrical spreading parameter, which is taken as '0.5' and '1' for surface waves and body waves, respectively, and Q_c represents the quality factor of coda waves. Equation (1) can be written as:

$$\ln\ (A(f,t),\ \ t) = \ln(S(f)) - \left(\frac{\pi f t}{Q_c}\right) \quad (2)$$

Relation (2) allows estimation of the Q_c from the slope of the straight line, fitted between $\ln(A(f, t))$ versus time t adopting least-squares method. According to Rautian and Khalturin (1978), the above relations are valid for lapse times greater than twice the S-wave travel time. The frequency-dependent relation of Q_c is described by the power law: $Q_c(f) = Q_0\ (f)^n$, where Q_0 is the value of Q_c at 1 Hz, and n represents the degree of frequency dependence of Q_c. The logarithm of this equation allows estimation of n and Q_0 using a simple linear regression.

2.1 Data set

A six-station local seismological network has been deployed around the Koldam located in the Himachal Lesser Himalaya (Fig. 1b. The local earthquake data collected through this network are interpreted to study the local seismicity and to map seismotectonic sources around the Koldam site. In this network, three short-period seismometers CMG-40TD1 (Guralp Systems Limited, UK) and two broadband seismometers CMG-3ESPC (Guralp Systems Limited, UK) are used as sensors to sense the three components of ground motion. The output from each sensor is coupled to a 24-bit portable data acquisition system (DL-24), and a global positioning system (GPS) is used to synchronize data samples to UTC or IST. The digital data are acquired at a rate of 100 samples per second (sps). In addition, one station is operated in an analog mode with short-period vertical-component seismometer L4C (Serceal, UK). Site characteristics and geographical coordinates of the recording stations are listed in Table 2.

Table 2 Site characteristics and geographical coordinates of the recording stations

Sl. no.	Name of station	Station code	Lat. (°N)	Long. (°E)	Elev. (Mts.)	Type of soil/rock
1	Sikandra	SKND	31.56°	76.81°	1589	Sandstone, shale and mudstone
2	Bandala	BAND	31.32°	76.78°	1328	Sandstone, shale and mudstone
3	Neri	NERI	31.22°	77°	1020	Slate, quartzite and carbonate rocks
4	Nihri	NIHR	31.59°	77.05°	1228	Phyllites, schists, gneiss and granitic rocks occur in near by areas
5	Kunho	KUNH	31.34°	77.2°	1558	Slate and dolomite
6	Gohar	GOHR	31.38°	77.03°	2082	Phyllites, schists, slate and quartzite

2.2 Data analysis

The digital data collected from all the stations have been converted to Seisan format with conversion programs available in SEISAN software (Havskov and Ottemoller 2003). Hypocenter parameters of local events have been estimated adopting HYPOCENTER program (Lienert et al. 1986; Lienert and Havskov 1995) and using the velocity model as listed in Table 3. The standard errors in the estimates of epicenter (ERH), focal depth (ERZ) and origin times (RMS residuals) are as follows: ERH $\leq$5.0 km; ERZ $\leq$5.0 km; and RMS $\leq$0.5 s. From May 2013 to March 2014, digital recordings of 41 local events from four stations (GOHR, KUNH, NERI and SKND) out of six stations are used in the study (Fig. 2). The digital data from Band and Nihri stations could not be used in this study because of low signal to noise ratio (SNR). All the local events occurred at epicentral distances of <100 km, and their magnitudes are in the range between 0.5 and 2.9.

A MATLAB code has been developed based on the single backscattering model of Aki and Chouet (1975) for the estimation of coda-Q. The guidelines of CODAQ subroutine of SEISAN have been followed for the development of the code (Havskov and Ottemoller 2003). The waveforms with SNRs above 3 are selected for analysis. The correlation coefficients are also used as a second selection criterion because Q values with small correlation coefficients lead to a poorly constrained Q–f relation and consequently a less reliable estimate of Q_0 and n values. It is suggested that correlation coefficient should be >0.7 to obtain the reliable values of Q_c. Further, the vertical components of coda waves have been used to estimate Q_c because it has been shown that the coda analysis is independent of the components of the ground motion analyzed (Hoshiba 1993).

Origin times and coda arrival times have been estimated from arrival times of P- and S-waves. Adopting Butterworth filter, the seismograms have been band-pass filtered at seven frequency bands, viz., 1–2, 2–4, 4–8, 6–12, 8–16, 12–24 and 16–32 Hz (Table 4). For each band-pass filtered earthquake time histories, signal is selected from coda arrival to coda duration considered for analysis. The elimination of contamination caused by direct S-wave is essential for reliable Q_c determination (Rautian and Khalturin 1978; Herraiz and Espinosa 1987). Therefore, direct S-waves from filtered earthquake time history are eliminated by taking the beginning of coda waves as twice the arrival time of S-wave from the origin time (Rautian and Khalturin 1978). The length of coda window is also important to get the stable solution. It is suggested that minimum window length should be 20 s (Havskov and Ottemoller 2005), and there is no maximum upper limit. In order to get stable and reliable solutions, three lapse time windows (20, 30 and 40 s) have been used. Coda waves selected in a specified time window are corrected for geometrical spreading. The corrected amplitudes are multiplied by 't^{α}' to account for geometrical spreading, and for local earthquakes, the value of $\alpha = 1$. The envelopes of the coda waves are estimated from root mean square (RMS) coda amplitudes computed using a moving window of 2 s with overlap of 1 s. The natural log of RMS amplitudes is plotted with t, and a linear

Table 3 Velocity model used in the study

Velocity (km/s)	Depth (km)
3.0	0.0
5.2	1.0
6.0	16.0
7.91	46.0

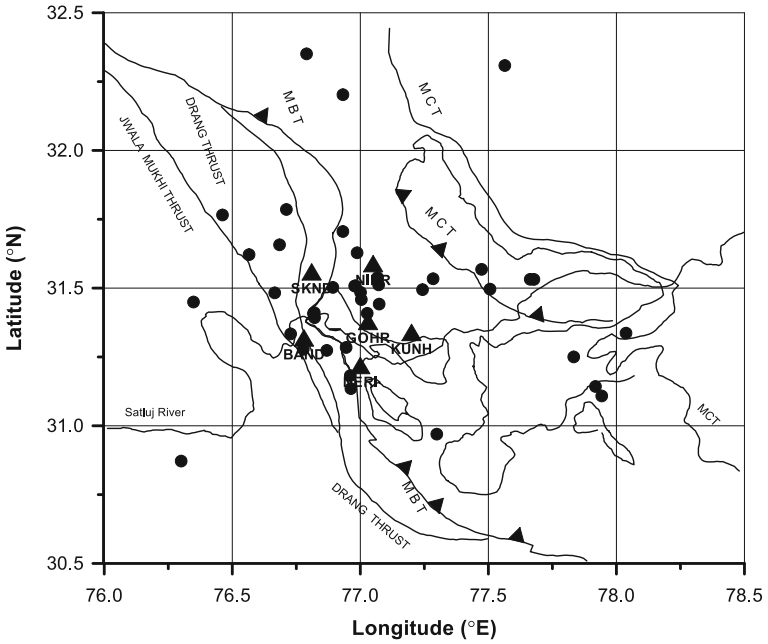

Fig. 2 Epicenters of events used in the study

Table 4 Various central frequencies with low-cut and high-cut frequency bands used for filtering

Low cutoff (Hz)	Central frequency (f) (Hz)	High cutoff (Hz)
1.00	1.50	2.00
2.00	3.00	4.00
4.00	6.00	8.00
6.00	9.00	12.00
8.00	12.00	16.00
12.00	18.00	24.00
16.00	24.00	32.00

equation is fitted to the data. The slope of the line provides coda-Q estimates at a particular central frequency (f_c) as depicted in Fig. 3.

3 Results and discussions

The frequency-dependent Q_c relations for each recording site as well as average relations for the Bilaspur region have been estimated. The spatial variation of estimated Q_c is studied, and its comparison with other seismically active regions of the India and world has been made. The 41 local events are grouped in three types according to the epicentral distance (R) range: near range ($R < 30$ km); medium range ($30 \leq R < 60$ km); and distant range ($R \geq 60$ km) (Table 5a–c).

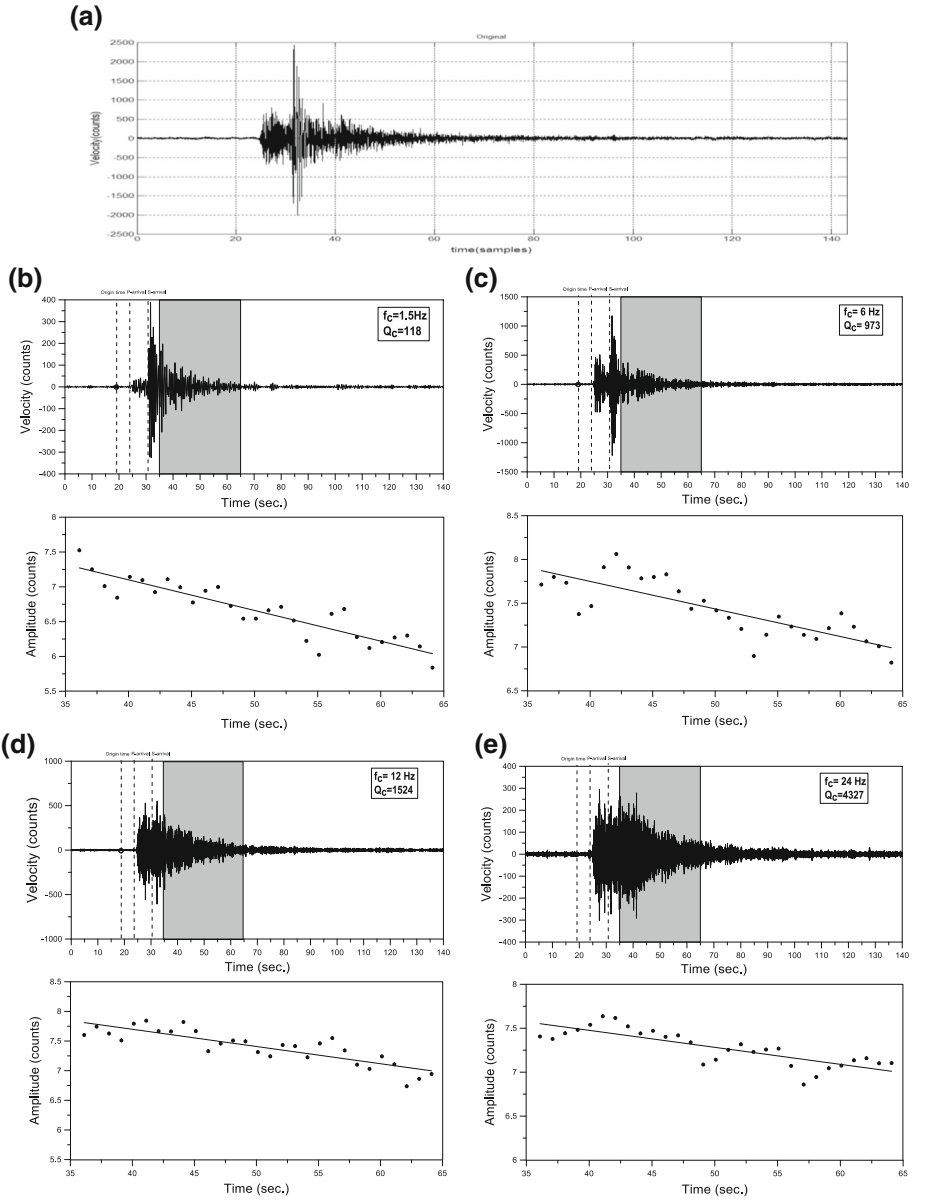

Fig. 3 Plot of event recorded at GOHR station on November 27, 2013. **a** Unfiltered data trace with coda window, **b–e** band-pass filtered displacement amplitudes of coda window at 1–2, 4–8, 8–16 and 16–32 Hz, respectively, and the RMS amplitude values multiplied with lapse time along with best square fits of selected coda window at central frequencies of 1.5, 6, 12 and 24 Hz, respectively. The Q_c is determined from the slope of best square line. *Abbreviations P*, *P*-wave arrival time; *S*, *S*-wave arrival time

Table 5 (a), (b), (c) shows the mean value with standard error at different frequencies and different lapse times (20, 30 and 40 s) for all stations which are distributed epicentral distance wise having (near range ($R < 30$ km), medium range ($30 \leq R < 60$ km) and distant range ($R \geq 60$ km)

Freq. (Hz)	Epi dis. (R < 30 km)		Epi dis. (30 ≤ R < 60 km)		Epi dis. (R ≥ 60 km)	
	Mean ± Stderr	*N*	Mean ± Stderr	*N*	Mean ± Stderr	*N*
(a) LTW 20 s						
1.5	87 ± 4	18	89 ± 10	6	96	1
3	166 ± 10	14			189 ± 11	2
6	543 ± 52	9	754 ± 133	6	680 ± 78	4
9	929 ± 46	9	1038 ± 99	13	1015 ± 74	11
12	1354 ± 108	10	1406 ± 160	13	1360 ± 76	19
18	2378 ± 237	12	1960 ± 109	13	2229 ± 137	17
24	2716 ± 236	13	2706 ± 242	13	3274 ± 260	15
(b) LTW 30 s						
1.5	98 ± 6	18	120 ± 10	8	130 ± 12	2
3	221 ± 12	18	440	1	292 ± 58	2
6	710 ± 45	15	769 ± 47	7	713 ± 102	5
9	1041 ± 38	18	1296 ± 78	17	1283 ± 75	17
12	1435 ± 53	23	1602 ± 93	18	1627 ± 68	20
18	2140 ± 71	21	2164 ± 86	16	2352 ± 93	19
24	2971 ± 123	17	2990 ± 216	14	3082 ± 165	14
(c) LTW 40 s						
1.5	118 ± 9	13	116 ± 6	7	166	1
3	318 ± 35	8	356 ± 85	3	254	1
6	880 ± 100	12	925 ± 98	7	1073 ± 151	5
9	1235 ± 88	18	1532 ± 77	17	1548 ± 68	20
12	1583 ± 70	18	1712 ± 77	17	1865 ± 65	18
18	2256 ± 111	16	2416 ± 113	17	2739 ± 178	16
24	3013 ± 132	14	2978 ± 122	11	3356 ± 162	14

Where $\pm\sigma$ represents the standard error and '*N*' is the number of earthquake used

3.1 Frequency and lapse time dependence of Q_c

The coda-Q estimated at central frequencies 1.5, 3, 6, 9, 12, 18 and 24 adopting three lapse time windows (LTWs) of 20-, 30- and 40-s durations is found to increase with increasing frequency and lapse time. We estimated frequency-dependent $Q(f)$ relations for each of the three distance ranges as well as for the entire data set because such Q_c relations are known to provide average attenuation characteristics of the medium properties of the localized regions (e.g., Mukhopadhyay et al. 2006). The mean values of Q_c with standard errors for 20-, 30- and 40-s LTWs, and for different distance, ranges with respect to each central frequency are listed in Table 5a–c. From Table 5a, it is evident that Q_c values are high at higher frequency ranges, which demonstrates the homogeneous character of the medium at deeper level. Similar patterns are observed from the Q_c values listed in Table 5b, c. A power law $Q_c = Q_0 f^n$, where Q_0 is the value of Q_c at 1 Hz and

n is frequency dependence coefficient (Aki 1980), is fitted to the data, for different LTWs. For 20-s LTW, the power law provided the average values of $Q_0 = 47 \pm 26$ and $n = 1.32 \pm 0.1$ for ($R < 30$ km); $Q_0 = 64 \pm 16$ and $n = 1.21 \pm 0.04$ for ($30 \leq R < 60$ km); and $Q_0 = 55 \pm 7.73$ and $n = 1.29 \pm 0.03$ for ($R \geq 60$ km), respectively. Similarly, the values of Q_0 and n have been estimated for 30- and 40-s LTWs are tabulated in Table 6.

The average estimates of Q_c obtained by taking the mean of Q_c values at different stations are listed in Table 7. Figure 4 depicts that at all the stations the variation of Q_c with frequency has a linear trend for 20-, 30- and 40-s LTWs. Furthermore, the Q_0 values are found to increase with lapse time for all stations, and n values are found to decrease with the LTW (Table 7). The increase in Q_c and decrease in n seem to signify the variation of attenuation character with depth as larger time window provides the effect of deeper part of the earth. Hence, it can be interpreted that when Q_c increases and n decreases, then heterogeneity decreases with depth in the study area (Mukhopadhyay and Tyagi 2007). According to the seismic zoning map of India, the study region falls in seismic zone V which represents the high seismicity of the region, and this is also reflected in the high estimated value of 'n.' For the study region, Q_c estimates follow the frequency-dependent relations: $Q_c = (70.3 \pm 20.27)\, f^{(1.23 \pm 0.05)}$ for 30-s LTW.

3.2 Spatial variation of Q_c

A large number of studies have demonstrated the dependence of Q_c with lapse time (e.g., Roecker et al. 1982; Kvamme and Havskov 1989; Ibanez et al. 1990; Woodgold 1994; Akinci et al. 1994; Gupta et al. 1996; Mukhopadhyay and Tyagi 2007). Further, the lapse time has been related to the area of sampling by coda waves. According to Pulli (1984), for a single scattering model, the coda wave attenuation represents the average decay of amplitudes of backscattered waves on the surface of ellipsoid with earthquake of source and station as foci. The coda waves at a station consist of the combination of several scattered phases, which do not represent a single ray. Hence, Q_c represents the average attenuation of the region comprises ellipsoidal volume with depth, $h = h_{av} + D2$, where $D2 = \sqrt{D1^2 - \Delta^2}$ is the small minor axis of ellipsoid for epicentral distance Δ and the average focal depth h_{av} of the events. The large semi-axis $D1$ is the surface projection of ellipsoid with hypocenter and station as foci and can be defined as $vt/2$. The average lapse time is given by the relations: $t = t_{st} + \frac{W}{2}$, where t_{st} is beginning of the lapse time

Table 6 Average value of quality factor Q_0 and n at different lapse time with distribution of epicentral distance

Lapse time (s)	Epi dis. ($R < 30$ km)		Epi dis. ($30 \leq R < 60$ km)		Epi dis. ($R \geq 60$ km)	
	Q_0	n	Q_0	n	Q_0	n
20	47 ± 26	1.32 ± 0.1	64 ± 16	1.21 ± 0.04	55 ± 7.73	1.29 ± 0.03
30	62 ± 9	1.24 ± 0.03	101 ± 20	1.09 ± 0.05	85 ± 18	1.16 ± 0.05
40	88 ± 17	1.15 ± 0.04	93 ± 40	1.16 ± 0.07	100 ± 40	1.16 ± 0.07

Table 7 Quality factor at each station and their average estimated values with different LTWs considered

Lapse time (s)	GOHR		KUNH		NERI		SKND	
	Q_0	n	Q_0	n	Q_0	n	Q_0	n
20	45.50 ± 8.68	1.34 ± 0.04	48.03 ± 12.0	1.27 ± 0.09	46.12 ± 13.95	1.34 ± 0.05	57.18 ± 33.5	1.30 ± 0.09
30	63.1 ± 13.74	1.22 ± 0.05	66.36 ± 14.35	1.22 ± 0.06	65.01 ± 28.48	1.25 ± 0.07	75.9 ± 20.62	1.20 ± 0.05
40	97.27 ± 42.70	1.12 ± 0.08	75.34 ± 14.22	1.23 ± 0.03	79.61 ± 46.82	1.22 ± 0.07	102.3 ± 35.12	1.14 ± 0.06

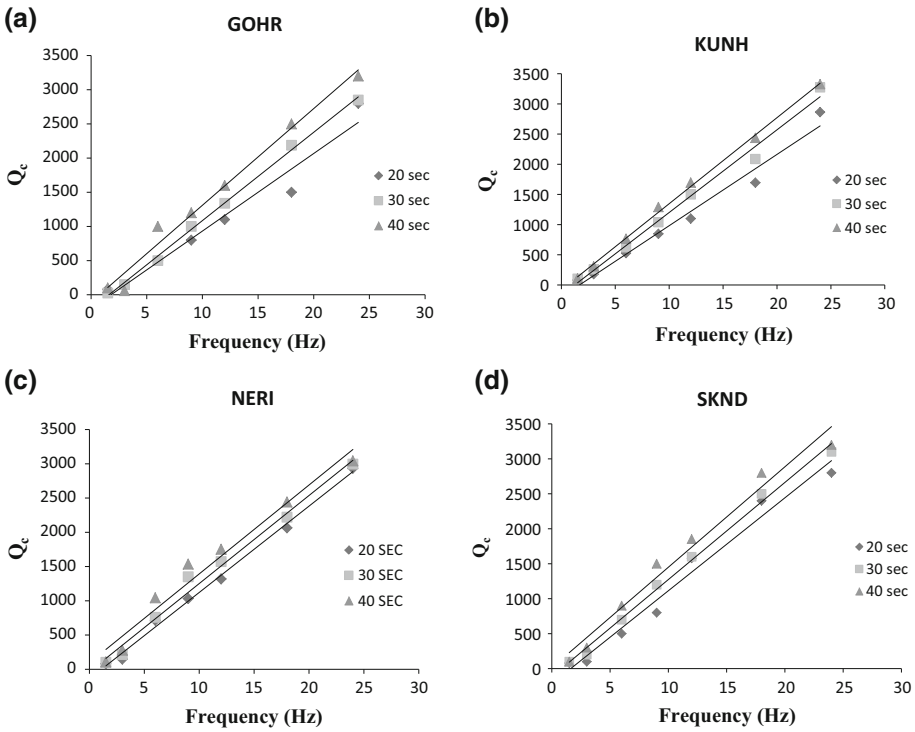

Fig. 4 Plots of quality factors and central frequencies for all the five stations (**a**–**d**) and average with linear regression frequency-dependent relationship, $Q_c = Q_0 f^n$ at different lapse time 20, 30 and 40 s

and W is the window length. The depths calculated for the ellipsoidal volume at different stations are given in Table 8. The increase in Q_c with lapse time is attributed to factors like considering nonzero source receiver distance, anisotropic scattering and assumption of single scattering model instead of multiple scattering (Woodgold 1994). For the three LTWs considered in this study, the starting time of coda wave is taken twice the S-wave travel time, and only backscattered waves are recorded in this time window (Aki and Chouet 1975). Further, for all the analyzed local events, the LTW length is <100 s, and the multiple scattering effects are not important for local events for lapse time <100 s (Gao et al. 1983). Hence, in the studied region, the variation of Q_c with lapse time is because of the variation of attenuation with depth and indicates that medium homogeneity increases with depth.

3.3 Comparison of Q_c with other regions of the India and the world

The single scattering or multiple scattering models have been used to estimate Q_c in different regions of the world (e.g., Aki and Chouet 1975; Sato 1977; Roecker et al. 1982; Pulli 1984; Wu 1985; Jin and Aki 1988; Havskov et al. 1989; Ibanez et al. 1990; Pujades et al. 1991; Canas et al. 1991; Akinci et al. 1994; Latchman et al. 1996; Zelt et al. 1999). In Fig. 5a, the Q_c estimates for Bilaspur region of the Himachal Lesser Himalaya are

Table 8 The maximum depth of ellipsoid volume

Station name	Average epicentral distance (Δ)	Average depth (h_{av})	Average lapse time (t)	Average S-wave velocity	$D1 = vt/2$ (km)	$D2 = \sqrt{D1^2 - \Delta^2}$	Depth $= h_{av} + D2$ (km)	Coverage area (km^2)
GOHR	41.6	13.8	43.5	3.3	71.78	58.49	72.29	13,183
KUNH	43.17	14.5	44.35	3.3	73.18	59.09	73.59	13,578
NERI	48.6	11.5	48.21	3.3	79.55	62.97	74.47	15,729
SKND	36.5	15.7	42.27	3.3	69.75	59.43	75.13	13,016
GOHR	41.6	13.8	43.5	3.3	71.78	58.49	72.29	13,183

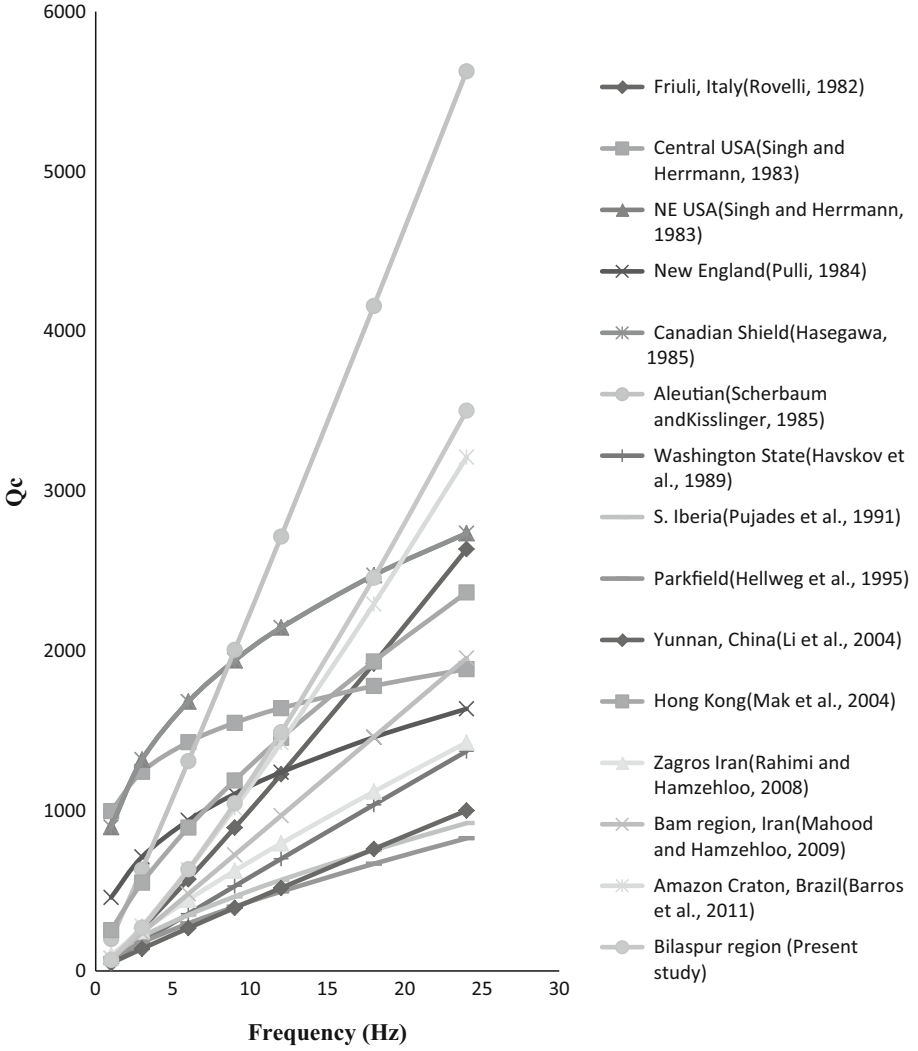

Fig. 5 **a**, **b** Comparison of Q_c values for Bilaspur region of the Himachal Lesser Himalaya with the existing Q studies worldwide and in India

compared with some of the regions of the world (Li et al. 2004; Havskov et al. 1989; Hellweg et al. 1995; Rovelli 1982; Mak et al. 2004; Mahood and Hamzehloo 2009; Rahimi and Hamzehloo 2008; Pujades et al. 1991; Barros et al. 2011). For comparison, frequency-dependent relations $Q_c = (70.3 \pm 20.27)\, f^{(1.23 \pm 0.05)}$ at 30-s LTW are considered, and it is found that average variation of Q_c for Bilaspur region is very close to Amazon Craton (Brazil). This may be due to the some kind of geological similarity between Bilaspur region and Amazon Craton (Brazil). The rock types of the Himachal Lesser Himalaya primarily comprise metasedimentary, sedimentary, igneous and metamorphic rocks,

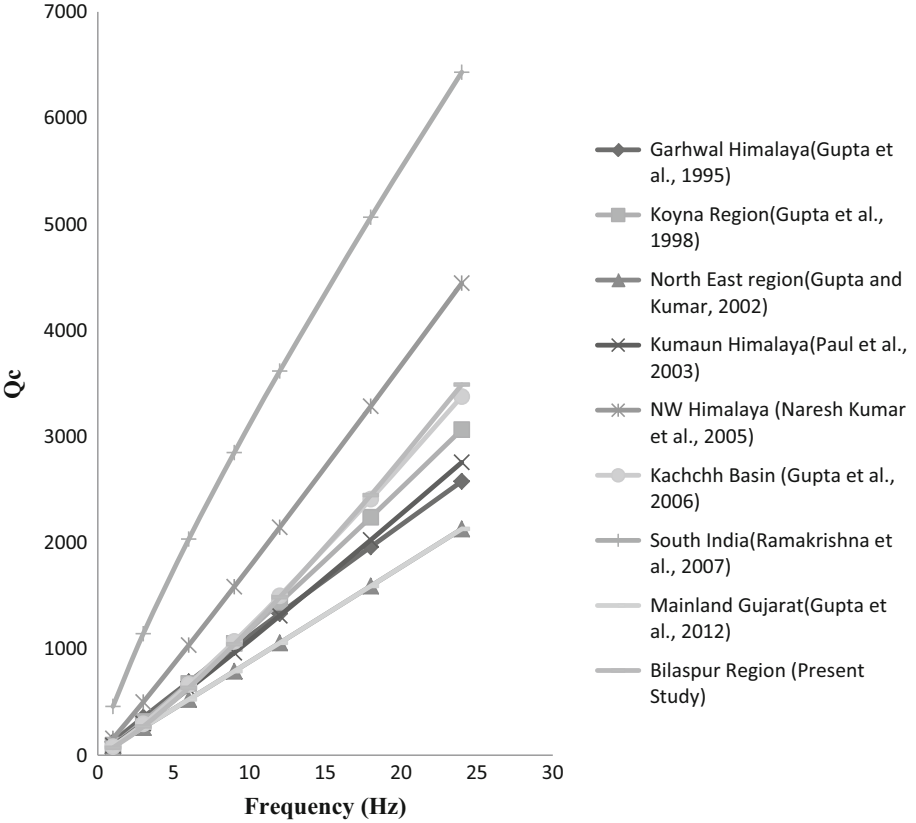

Fig. 5 continued

whereas the Amazon Craton of Brazil comprises of granitic rocks and Phanerozoic terrains with sedimentary rocks of the Parecis basin.

The Himalaya is seismically and tectonically very active. Since 1995, several studies on the estimation of seismic wave attenuation were undertaken (e.g., Gupta et al. 1995, 1998, 2012; Gupta and Kumar 2002; Paul et al. 2003; Kumar et al. 2005; Ramakrishna et al. 2007). Figure 5b shows the comparison of Q_c estimates of the Bilaspur region with the Q_c estimates from various other Indian regions. The variation of Q_c with frequency for the Bilaspur region is almost similar to that of Kachchh region. Table 9 shows the comparison of Q_c at 1 Hz (Q_0) for the Bilaspur region with the other Indian regions. It is found that 'Q_0' has minimum value for the Bilaspur region. This means that the Bilaspur region is the most attenuating among the regions compared. The 'n' value for the Bilaspur region is also maximum than any other Indian region and some of the regions of the world (Table 9). This indicates that the Bilaspur region is highly heterogeneous in character and that the lowest 'Q_0' is observed for this Indian region. This may be due to the presence of criss-crossed fractures, intrusions and heterogeneities of varying scales attributed to the Himalaya orogeny.

Table 9 Comparison of attenuation quality factor 'Q_0' and 'n' with other regions of the world and India

Regions	Q_o	n	References
World			
Friuli, Italy	80	1.1	Rovelli (1982)
NE, USA	900	0.35	Singh and Herrmann (1983)
Central USA	1000	0.2	Singh and Herrmann (1983)
New England	460	0.4	Pulli (1984)
Aleutian	200	1.05	Scherbaum and Kisslinger (1985)
Canadian Shield	900	0.35	Hasegawa (1985)
Washington State	63	0.97	Havskov et al. (1989)
S. Iberia	100	0.7	Pujades et al. (1991)
Parkfield	79	0.74	Hellweg et al. (1995)
Hong Kong	256	0.7	Mak et al. (2004)
Yunnan, China	49	0.95	Li et al. (2004)
Zagros Iran	99	0.84	Rahimi and Hamzehloo (2008)
Bam region, Iran	79	1.01	Mahood and Hamzehloo (2009)
Amazon Craton, Brazil	78	1.17	Barros et al. (2011)
Indian region			
Garhwal Himalaya	126	0.95	Gupta et al. (1995)
Koyna region	96	1.09	Gupta et al. (1998)
Northeast region	86	1.01	Gupta and Kumar (2002)
Kumaun Himalaya	92	1.07	Paul et al. (2003)
NW Himalaya	158	1.05	Naresh Kumar et al. (2005)
Kachchh Basin	82	1.17	Gupta et al. (2006)
South India	460	0.83	Ramakrishna et al. (2007)
Mainland Gujarat	87	1.01	Gupta et al. (2012)
Bilaspur region of Himachal Lesser Himalaya	70	1.23	Present study

4 Conclusion

The frequency-dependent coda-Q relations for the Bilaspur region of the Himachal Lesser Himalaya have been estimated considering LTWs of 20-, 30- and 40-s durations. The Q_c estimates are computed in the frequency range from 1.5 to 24 Hz, using a data set of 41 local events. The variation of Q_c with distance is investigated by dividing the data set into near ($R < 30$ km), medium ($30 \leq R < 60$ km) and distant ranges ($\geq$60 km), respectively.

For 20-s LTW, the Q_c estimates vary from 87 ± 4 (at 1.5 Hz) to 2716 ± 236 (at 24 Hz) for R < 30 km; 89 ± 10 (at 1.5 Hz) to 2706 ± 242 (at 24 Hz) for $30 \leq R < 60$ km; and 96 (at 1.5 Hz) to 3274 ± 260 (at 24 Hz) for $R \geq 60$ km. Similarly, for 30-s LTW, the Q_c estimates vary from 98 ± 6 (at 1.5 Hz) to 2971 ± 123 (at 24 Hz) for $R < 30$ km; 120 ± 10 (at 1.5 Hz) to 2990 ± 216 (at 24 Hz) for $30 \leq R < 60$ km; and 130 ± 12 (at 1.5 Hz) to 3082 ± 165 for $R \geq 60$ km), while for 40-s LTW, Q_c estimates vary from 118 ± 9 (at 1.5 Hz) to 3013 ± 132 (at 24 Hz) for $R < 30$ km; 116 ± 6 (at 1.5 Hz) to 2978 ± 122 (at 24 Hz) for $30 \leq R < 60$ km; and 166 (at 1.5 Hz) to 3356 ± 162 (at

24 Hz) for $R \geq 60$ km. It is found that Q_c values are high at higher frequencies and show the homogeneity at deeper zones.

For 30-s LTW, the frequency-dependent relations $Q_c = (70.3 \pm 20.27) f^{(1.23 \pm 0.05)}$ have been obtained for the Bilaspur region considering entire data set. Comparison of Q_c estimates for the Bilaspur region with some of the seismically active region of the world has shown that the average variation of Q_c for this region is very close to Amazon Craton (Brazil) due to similar lithologic setup. From the comparison of 'Q_0' and 'n' obtained for the Bilaspur region with other Indian regions, it is found that the Bilaspur region is most attenuating and highly heterogeneous in nature. Further, the variation of Q_c with frequency for the Bilaspur region is almost similar to that of Kachchh region. The various attenuation relations developed for the Bilaspur region shall be useful for computing earthquake source parameters, simulating earthquake strong ground motions and for seismic hazard assessment of the region.

Acknowledgments The authors are thankful to the National Thermal Power Corporation (NTPC) Kol dam, Himachal Pradesh, for sponsoring the project under which data were collected. Thanks are due to Head, the Department of Earthquake Engineering, Indian Institute of Technology, Roorkee, for providing facilities to carry out this research work.

References

Aki K (1969) Analysis of seismic coda of local earthquakes as scattered waves. J Geophys Res 74:615–631

Aki K (1980) Attenuation of shear waves in the lithosphere for frequencies from 0.05 to 25 Hz. Phys Earth Planet Inter 21:50–60

Aki K, Chouet B (1975) Origin of coda waves: source, attenuation and scattering effects. J Geophys Res 80:3322–3342

Akinci A, Taktak AG, Ergintav S (1994) Attenuation of coda waves in Western Anatolia. Phys Earth Planet Inter 87:155–165

Ambeh WB, Fairhead JD (1989) Coda-Q estimates in the Mount Cameroon volcanic region, West Africa. Bull Seismol Soc Am 79:1589–1600

Ambraseys N, Bilham R (2000) A note on the Kangra Ms = 7.8 earthquake of 4 Apr. Curr Sci 79(1):45–50

Atkinson GM, Meeru RF (1992) The shape of ground motion attenuation curves in Southeastern Canada. Bull Seismol Soc Am 82:2014–2031

Barros LV, Assumpcao M, Quintero R, Ferreira VM (2011) Coda wave attenuation in the Parecis Basin Amazon craton—Brazil—sensitivity to basement depth. J Seismol 15:391–409

Calvet M, Sylvander M, Margerin L, Villasenor A (2013) Spatial variations of seismic attenuation and heterogeneity in the Pyrenees: coda Q and peak delay time analysis. Tectonophysics 608:428–439

Canas JA, Pujades L, Badal J, Payo G, Demiguel F, Vidal F, Alguacil G, Ibanez J, Morales J (1991) Lateral variation and frequency dependence of coda-Q in the southern part of Iberia. Geophys J Inter 107:57–66

Catherine RDW (1990) Estimation of Q in Eastern Canada using coda waves. Bull Seismol Soc Am 80:411–429

Demets C, Gordon RG, Argus DF, Stein S (1990) Current plate motions. Geophys J Inter 101:425–478

Dobrynina AA (2011) Coda-wave attenuation in the Baikal rift system lithosphere. Phys Earth Planet Inter 188:121–126

Gao LS, Biswas NN, Lee LC, Aki K (1983) Effects of multiple scattering on coda waves in three dimensional medium. Pure Appl Geophys 121:3–15

GSI (2000). Seismotectonic Atlas of India and its Environs. In: Narula PL, Acharya SK, Banerjee J (eds) Geol Surv India, Sp Pub

Gupta SC, Kumar A (2002) Seismic wave attenuation characteristics of three Indian regions—a comparative study. Curr Sci 82:407–413

Gupta SC, Singh VN, Kumar A (1995) Attenuation of coda waves in the Garhwal Himalaya, India. Phys Earth Planet Inter 87:247–253

Gupta SC, Kumar A, Singh VN, Basu S (1996) Lapse-time dependence of Q_c in the Garhwal Himalaya. Bull Indian Soc Earthq Technol 33:147–159

Gupta SC, Teotia SS, Rai SS, Gautam N (1998) Coda Q estimates in the Koyna region, India. Pure Appl Geophys 153:713–731
Gupta SC, Kumar A, Shukla AK, Suresh G, Baidya PR (2006) Coda Q in the Kachchh basin, western India using aftershocks of the Bhuj earthquake of January 26, 2001. Pure Appl Geophys 163:1583–1595
Gupta AK, Sutar AK, Chopra S, Kumar S, Rastogi BK (2012) Attenuation characteristics of coda waves in Mainland Gujarat (India). Tectonophysics 530:264–271
Hasegawa H (1985) Attenuation of Lg wave in the Canadian Shield. Bull Seismol Soc Am 75:1569–1582
Havskov J, Ottemoller L (2003) SEISAN: the earthquake analysis softwares for Windows, Solaris and Linux, Version 8.0. Institute of Solid Earth Physics, University of Bergen, Norway
Havskov J, Ottemoller L (2005) SEISAN (version 8.1): the earthquake analysis software for Windows, Solaris, Linux, and Mac OSX Version 8.0. 254
Havskov J, Malone S, Mcclurg D, Crosson R (1989) Coda Q for the state of Washington. Bull Seismol Soc Am 79:1024–1038
Hellweg M, Spandich P, Fletcher JB, Baker LM (1995) Stability of coda-Q in the region of Parkfield, California: view from the U.S. Geological Survey Parkfield Dense Seismograph Array. J Geophys Res 100:2089–2102
Herraiz M, Espinosa AF (1987) Coda waves: a review. Pure Appl Geophys 125:499–577
Hoshiba M (1993) Separation of scattering attenuation and intrinsic absorption in Japan using the multiple lapse time window analysis of full seismogram envelope. J Geophys Res 98:15809–15824
Ibanez JM, Delpezzo E, Demiguel F, Herraiz M, Alguaicil G, Morales J (1990) Depth dependent seismic attenuation in the Granada Zone (Southern Spain). Bull Seismol Soc Am 80:1232–1244
IS (2002), IS 1893–2002 (Part 1) Indian standard criteria for earthquake resistant design of structures, part 1—general provisions and buildings. Bureau of Indian Standards, New Delhi
Jin A, Aki K (1988) Spatial and temporal correlation between coda Q and seismicity in China. Bull Seismol Soc Am 78:741–769
Johnston DH, Toksöz MN (eds) (1981) Seismic wave attenuation. Society of Exploration Geophysicists 1–5
Kopnichev YF (1977) The role of multiple scattering in the formation of seismogram's tail, Izvestiya. Phys Solid Earth 13:394–398
Kumar S, Mahajan AK (1990) Studies of intensities of 26th April, 1986 Dharamsala earthquake and associated tectonics. Geol Soc India 35:213–219
Kumar N, Parvez IA, Virk HS (2005) Estimation of coda waves attenuation for NW Himalayan region using local earthquakes. Research report CM 0404, C MMACS, India
Kumar CHP, Sharma CSP, Sekhar M, Chadha RK (2007) Attenuation studies based on local earthquake coda waves in the Southern Indian Peninsular shield. Nat Hazard 40(3):527–536
Kvamme LB, Havskov J (1989) Q in southern Norway. Bull Seismol Soc Am 79:1575–1588
Latchman JL, Ambeh WB, Lynch LL (1996) Attenuation of seismic waves in the Trinidad and Tobago area. Tectonophysics 253:111–127
Le Fort P (1975) Himalayas: the collided range. Present knowledge of the continental arc. Am J Sci 275-A:1–44
Li BJ, Qin JZ, Qian XD, Ye JQ (2004) The coda attenuation of the Yaoan area in Yunnan Province. Acta Seismol Sin 17(1):47–53
Lienert BR, Havskov J (1995) A computer program for locating earthquakes both locally and globally. Seismol Res Lett 66(5):26–36
Lienert BR, Berg E, Frazer LN (1986) HYPOCENTER: an earthquake location method using centered, scaled, and adaptively damped least squares. Bull Seismol Soc Am 76(3):771–783
Mahood M, Hamzehloo H (2009) Estimation of coda wave attenuation in East Central Iran. J Seismol 13:125–139. doi:10.1007/s10950-008-9130-2
Mak S, Chan LS, Chandler AM, Koo RCH (2004) Coda Q estimates in the Hong Kong region. J Asian Earth Sci 24:127–136
Mandal P, Rastogi BK (1998) A frequency-dependent relation of coda Qc for Koyna-Warna region, India. Pure Appl Geophys 153:163–177
Mandal P, Padhy S, Rastogi BK, Satyanarayana VS, Kousalya M, Vijayraghavan R, Srinvasa A (2001) Aftershock activity and frequency dependent low coda Qc in the epicentral region of the 1999 Chamoli earthquake of Mw 6.4. Pure appl Geophys 158:1719–1735
Molnar P, Chen WP (1983) Focal depths and fault-plane solutions of earthquakes under the Tibetan Plateau. J Geophys Res 88:1180–1196
Mukhopadhyay S, Tyagi C (2007) Lapse time and frequency-dependent attenuation characteristics of coda waves in the Northwestern Himalayas. J Seismol 11(2):149–158
Mukhopadhyay S, Tyagi SC, Rai SS (2006) The attenuation mechanism of seismic waves for NW Himalaya. Geophys J Int 167:354–360

Nakata T (1989) Active faults of the Himalaya of India and Nepal. In: Malinconico LL Jr, Lillie RJ (eds) Tectonics of the Western Himalaya. Geol Soc America Spl Paper (Geological Society of America, Colorado, 1989), 232:243–264

Pandit P, Kumar D, Muralimohan TR, Niyogi K, Das SK (2011) Estimation of seismic Q using a non-linear (Gauss-Newton) regression. Geohorizons 19–23

Paul A, Gupta SC, Pant CC (2003) Coda Q estimates for Kumaon Himalaya. Proc Ind Acad Sci (Earth Planet Sci) 112:569–576

Pujades L, Canas JA, Egozcue JJ, Puigvi MA, Pous J, Gallart J, Lana X, Casas A (1991) Coda Q distribution in Iberian Peninsula. Geophys J Int 100:285–301

Pulli JJ (1984) Attenuation of coda waves in New England. Bull Seismol Soc Am 74:1149–1166

Raghukanth STG, Semala SN (2009) Modelling of strong motion data in Northeastern India; Q, stress drop and site amplification. Bull Seismol Soc Am 99(2A):705–725

Rahimi H, Hamzehloo H (2008) Lapse time and frequency-dependent attenuation of coda waves in the Zagros continental collision zone in Southwestern Iran. J Geophys Eng 5:173–185

Ramakrishna RCV, Seshamma NV, Mandal P (2007) Attenuation studies based on local earthquake coda waves in the southern Indian peninsular shield. Nat Hazards 40(3):527–536

Rautian TG (1976) Role of source and medium in the formation of seismic oscillations near local earthquakes. Investigations of the physics of earthquakes. Nauka Publishing House, Moscow, pp 27–55 **in Russian**

Rautian TG, Khalturin VI (1978) The use of the coda for the determination of the earthquake source spectrum. Bull Seismol Soc Am 68:923–948

Roecker SW, Tucker B, King J, Hartzfield D (1982) Estimates of Q in Central Asia as a function of frequency and depth using the coda of locally recorded earthquakes. Bull Seismol Soc Am 72:129–149

Rovelli A (1982) On the frequency dependence of Q in Friuli from short period digital records. Bull Seismol Soc Am 72:2369–2372

Sahin S (2008) Lateral variations of coda Q and attenuation of Seismic waves in Southwest Anatolia. J Seismol 12:367–376

Sato H (1977) Energy propagation including scattering effects: single isotropic approximation. J Phys Earth 25:27–41

Sato H, Fehler MC (1998) Seismic wave propagation and scattering in the Heterogeneous Earth. Springer, New York

Saxena MN (1971) Geological classification and the tectonic history of the Himalaya. Proc Ind Nat Sci Acad 37:228–254

Scherbaum F, Kisslinger C (1985) Coda *Q* in the Adak seismic zone. Bull Seismol Soc Am 75:615–620

Seeber L, Armbruster JG, Quitt-Meyer RC (1981) Seismicity and continental subduction in the Himalayan arc. In Zagros, Hindu-Kush, Himalaya, Geodynamic Evolution. Geodyn Am Geophys Union 3:215–242

Sharma B, Gupta AK, Devi DK, Kumar D, Teotia SS, Rastogi BK (2008) Attenuation of high frequency seismic waves in Kachchh region, Gujarat, India. Bull Seismol Soc Am 98:2325–2340

Singh SK, Herrmann RB (1983) Regionalization of crustal coda Q in the continental United States. J Geophys Res 88:527–538. doi:10.1029/JB088iB01p00527

Singh S, Jain AK, Sinha P, Singh VN, Srivastava LS (1976) The Kinnaur earthquake of January 19, 1975: a field report. Bull Seismol Soc Am 66(3):887–901

Srikanita SV, Bhargava ON (1998) Geology of Himachal Pradesh: Bangalore. Geologic Society of India

Srivastava HN, Dubey RK, Raj H (1987) Space and time variation in seismicity patterns preceding two earthquakes in the Himachal Pradesh, India. Tectonophys 113:69–77

Thakur A, Sharma D, Kumar P, Gupta N, Dhiman P (2014) Expected seismic performance of buildings located in Waknaghat and Kandaghat area of Solan, District. Int J Sci Eng Res 5:2229–5518

Valdiya KS (1979) An outline of the structural set-up of the Kumaon Himalaya. J Geol Soc India 20:145–157

Valdiya KS (1987) Trans-Himadri Thrust and domal upwards immediately south of collision zone and tectonic implications. Curr Sci 56:200–209

Valdiya KS (1989) Trans-Himadri intracrustal fault and basement upwards south of the Indus-Tsangpo Suture Zone. Geol Soc Am Spec 153–168

Valdiya KS, Joshi DD, Sanwal R, Tandon SK (1984) Geomorphologic envelopment across the active main boundary Thrust, an example from the Nainital Hills in Kumaun Himalaya. J Geol Soc India 25(12):761–774

Woodgold C (1994) Coda-Q in Charlevoix, Quebec, Region. Lapse time dependence and Spatial and temporal comparisons. Bull Seismol Soc Am 84:1123–1131

Wu RS (1985) Multiple scattering and energy transfer of seismic waves-separation of scattering effect from intrinsic attenuation—I. Theoretical modelling. Geophys J R Astr Soc 82:57–80
Zelt BC, Dotzev NT, Ellis RM, Roger GC (1999) Coda Q in Southwestern British Columbia, Canada. Bull Seismol Soc Am 89:1083–1093